Optical properties of Cr^{3+} –doped oxides: Different behavior of two centers in alexandrite

J. M. García-Lastra,[1] J. A. Aramburu,[2] M. T. Barriuso,[1] and M. Moreno[2]
[1]*Departamento de Física Moderna, Universidad de Cantabria, 39005 Santander, Spain*
[2]*Departamento de Ciencias de la Tierra y Física de la Materia Condensada, Universidad de Cantabria, 39005 Santander, Spain*
(Received 29 May 2006; published 21 September 2006)

This work is aimed at explaining the different color exhibited by the two Cr^{3+} centers in the alexandrite gemstone as well as ruby and emerald. Although the average Cr^{3+}-O^{2-} distance in ruby, emerald, and the C_s center in alexandrite is known to be practically the same, it is shown that the different values of the ligand field parameter $10Dq$ of the four Cr^{3+} centers mainly come from the electrostatic potential of the rest of lattice ions, $V_R(\mathbf{r})$, seen by the CrO_6^{9-} complex where active electrons are localized. This $V_R(\mathbf{r})$ potential, which strongly depends on the point symmetry group around the impurity, leads to an additional contribution to $10Dq$ not considered in the traditional ligand field theory. While for the C_s center ($10Dq$=2.19 eV) and ruby ($10Dq$ =2.24 eV), $V_R(\mathbf{r})$ has a similar shape along any Cr^{3+}-O^{2-} direction this is no longer true for the C_i center in alexandrite where the highest $10Dq$ value (equal to 2.53 eV) is measured.

DOI: 10.1103/PhysRevB.74.115118 PACS number(s): 71.55.−i, 71.15.Mb, 61.72.Ji, 91.60.Mk

I. INTRODUCTION

A great deal of work has been focused on ruby (Al_2O_3:Cr^{3+}), emerald ($Be_3Si_6Al_2O_{18}$:Cr^{3+}), and alexandrite ($BeAl_2O_4$:Cr^{3+}).[1–3] These doped materials are reference systems among gemstones and also in the realm of impurities in insulating materials. Indeed the first operating laser was made using the ruby emission which is currently used for measuring the applied pressure in diamond anvil cells.[4] Tunable lasers employing the luminescence of alexandrite and emerald have also been built.[3,5]

From a fundamental standpoint, it is crucial to understand the origin of the different optical properties exhibited by the three referred gemstones.[1–3,6–9] In Table I, the energy E_1 of the ${}^4A_{2g}(t_{2g}{}^3) \rightarrow {}^4T_{2g}(t_{2g}{}^2e_g)$ optical absorption maximum (in octahedral notation) together with the energy, E_{em}, of the sharp ${}^2E_g(t_{2g}{}^3) \rightarrow {}^4A_{2g}(t_{2g}{}^3)$ transition for the three gemstones are collected. As a salient feature it should be noticed that in the case of $BeAl_2O_4$ there are two nonequivalent Al^{3+} sites, thus leading to the existence of two different Cr^{3+} centers in alexandrite.[7–15] The local symmetry of the dominant center has only a mirror plane (C_s center) while the second one exhibits inversion symmetry (C_i center). For the sake of completeness the value of the *average* distance, R_H, between Al^{3+} and the six nearest O^{2-} ions is also gathered in Table I for Al_2O_3, $Be_3Si_6Al_2O_{18}$, and the two sites in $BeAl_2O_4$.[6,10,11]

Looking at data of Table I, remarkable differences among the measured values of E_1 are found. For instance, E_1 for the C_i center in alexandrite is 27% higher than in the case of emerald. Similarly, E_1 for ruby is found to be 12% higher when compared to the figure in $Be_3Si_6Al_2O_{18}$:Cr^{3+}, a fact which is behind the different color displayed by such gemstones. By contrast, the experimental values reported for E_{em} corresponding to the four centers (Table I) are coincident within 2%.

An explanation of the remarkable differences exhibited by the E_1 value of the four centers in Table I has been attempted[16,1–3,6] through the traditional ligand field theory,[17] which can be applied provided active electrons are *localized* in the MX_N complex formed by the impurity, M, and the N nearest anions. In these cases it has been assumed that electronic properties associated with an impurity can be well explained considering only the *isolated* MX_N molecule at the right equilibrium M-X distance, R. It should be noticed that this distance reflects the chemical pressure exerted by the host lattice upon the MX_N complex.[18]

According to this view, the different E_1 values reported in Table I would imply different R values for the involved systems. More precisely, the energy E_1 of the ${}^4A_{2g} \rightarrow {}^4T_{2g}$ transition is just equal to $10Dq$.[17] Within the traditional ligand field theory, $10Dq$ is assumed to depend *only* on the equilibrium impurity-ligand distance, R, through the law

$$10Dq = KR^{-n}, \tag{1}$$

and the exponent n is found to lie typically between 4 and 6 for transition metal impurities in octahedral coordination.[18] Therefore, if this explanation is the right one, E_1 values in Table I would imply[16] R(emerald)−R(ruby)=5 pm, or R(emerald)−R(alexandrite;C_i center)=10 pm, taking n=4.5.[19] However, these conclusions are hard to accept when considering available data on impurity-ligand distances.[18] Let us consider two host lattices with the same ligand and coordination number but different R_H values. If ΔR_H denotes such a difference it is found that when the host cation is replaced by the same substitutional impurity then $\Delta R < \Delta R_H$. Here ΔR means the difference of R values found in two lattices. Assuming ΔR=5 pm as the difference between emerald and ruby, this figure is certainly higher than $|\Delta R_H|$=1 pm derived under the comparison of $Be_3Si_6Al_2O_{18}$ and Al_2O_3 in Table I. A great support to this reasoning has been provided by recent extended x-ray absorption fine structure (EXAFS) measurements carried out on ruby and emerald[6,20] demonstrating that the R value for both gemstones is the same within the experimental uncertainty (±1 pm). Along this line, EXAFS data also reveal that R increases only 1 pm on going from Al_2O_3:Cr^{3+} to Cr_2O_3.[21]

A simple explanation on the puzzling difference in color exhibited by ruby and emerald has recently been proposed.[22] It has been argued that although active electrons are

TABLE I. Experimental peak energies (in cm^{-1} units) of the first absorption, E_1, and emission, E_{em}, transitions corresponding to the four centers analyzed in this work. Experimental values of the averaged Al^{3+}-O^{2-} distances, R_H, (in pm) for each pure lattice are also given.

System	Symmetry of the center	R_H	$E_1=10Dq$ $^4A_{2g}\rightarrow{}^4T_{2g}$	E_{em} $^2E_g\rightarrow{}^4A_{2g}$	References
Ruby	C_3	191.3	18070	14420	1–3 and 6
Emerald	D_3	190.6	16130	14690	1, 2, and 6
Alexandrite	C_s	193.7	17700	14750	3 and 7–11
Alexandrite	C_i	189.0	20410	14450	3 and 7–11

localized,[23] this does not necessarily mean that electronic properties can be explained considering *only* the CrO_6^{9-} complex *in vacuo* at the right equilibrium distance. Indeed, such a complex is never isolated but embedded in an ionic lattice and thus also subject to an internal electric field due to the rest of lattice ions. It has been shown that this electric field on the CrO_6^{9-} complex (strongly dependent on the point symmetry group around the impurity) produces an additional contribution to $10Dq$ that is actually responsible for the difference in color between ruby and emerald.[22]

If this idea is right, it should also be possible to account for the $10Dq$ values corresponding to the two centers observed in alexandrite. In particular the $E_1=2.53$ eV value measured for the C_i center in the alexandrite is about 10% higher than the figure reported for the C_s center and also ruby (Table I).

The present work is aimed at exploring this relevant issue following the same procedure recently employed for ruby and emerald.[22] Details on calculations are briefly commented on in the next section, while main results on C_s and C_i centers in alexandrite are reported in Sec. III and compared to those on $Al_2O_3:Cr^{3+}$ and $Be_3Si_6Al_2O_{18}:Cr^{3+}$.

II. THEORETICAL

A main goal of this work is to explore whether the different $10Dq$ values for the four Cr^{3+} centers (Table I) can be accounted for by simply considering the CrO_6^{9-} complex though subject to the corresponding electrostatic potential, $V_R(\mathbf{r})$, arising from the rest of lattice ions. For investigating this issue calculations in the framework of the density functional theory (DFT) have been performed by means of the ADF code.[24] For every system, $10Dq$ has been computed for the complex *in vacuo* as well as including the effects of $V_R(\mathbf{r})$. The same functional and basis set are employed for calculating the four Cr^{3+} centers of Table I. The generalized gradient approximation (GGA) exchange-correlation energy was computed using the Perdew-Wang functional, PW91.[25] It was verified that the obtained results are almost independent on the used functional. All atoms except oxygen were described through basis sets of TZP [triple-ζ Slater-type orbitals (STO) plus one polarization function] quality given in the program database, and the core electrons ($1s$-$3p$ for Cr and $1s$ for O) were kept frozen. The description for oxygen ions providing better agreement with experimental findings for ruby[22] and for Fe^{3+}-O^{2-} pairs in $KMgF_3$ (Ref. 26) was shown to be obtained through the DZP (double-ζ STO plus one polarization function) basis set. It should be stressed here that main differences between ruby and emerald were always reproduced through other basis set.[22] Calculations have been carried out at the equilibrium geometry of the four Cr^{3+} centers in Table I. Available information on the local symmetry, Al^{3+}-O^{2-} distances in the host lattice as well as actual Cr^{3+}-O^{2-} distances in the doped material is collected in Table II. It can be noticed that the R value derived through EXAFS measurements for ruby and emerald[6,20,21] is the same within the experimental uncertainty (±1 pm). The positive $R-R_H$ value found for both gemstones is consistent with the smaller ionic radius of Al^{3+} when compared to that of Cr^{3+}. The Cr^{3+}-O^{2-} distances given in Table II for the C_s center in alexandrite have been calculated by Watanabe and Ogasawara[27] and lead to an R value practically identical to that for ruby and emerald. As no precise structural information on the C_i center in alexandrite is at present available the Cr^{3+}-O^{2-} distances for this center in Table II have been derived taking into account the results for the other three centers and assuming 197 pm. $10Dq$ has always been derived following the average of configuration procedure given in Refs. 29 and 30. The center of gravity of small splittings undergone by the t_{2g} and e_g orbitals in low symmetries has been taken into account when deriving $10Dq$.

The electrostatic potential $V_R(\mathbf{r})$ coming from all ions of Al_2O_3, $Be_3Si_6Al_2O_{18}$, or $BeAl_2O_4$ crystals lying outside the CrO_6^{9-} unit has been obtained through the following two-step procedure.[28] In a first step, this potential has been calculated using Ewald's method in a great number of points inside a sphere bigger than the cluster. In this calculation the nominal ionic charges have been used, due to the high ionic character of the lattices and the weak dependence of results on the actual values of charges.[22] In a second step, the potential inside the sphere has been reproduced using about 150 effective charges lying outside the sphere. These charges are located at lattice positions although the value of charges itself is fitted in order to reproduce the right potential inside the sphere. Finally, these effective charges were placed into the ADF calculations.

III. RESULTS AND DISCUSSION

The $10Dq$ values for the four centers of Table I calculated at the equilibrium Cr^{3+}-O^{2-} distances are collected in Table III and compared to experimental values. In this table, the

TABLE II. Experimental values of the actual Al^{3+}-O^{2-} distances, R_H, and Cr^{3+}-O^{2-} distances, R, for the four centers studied in this work. The number of bonds of each type is given in parenthesis. Average values are in italic. All values are given in pm.

Lattice	Symmetry of the center	R_H	Reference	R	Reference
Al_2O_3	C_3	185.6 (3)		192.0 (3)	
		196.9 (3)	6	201.0 (3)	6, 20, and 21
		191.3		*196.5*	
$Be_3Si_6Al_2O_{18}$	D_3	190.6 (6)	6	197.5 (6)	6
$BeAl_2O_4$	C_s	186.1 (1)		192 (1)	
		189.3 (2)		195 (2)	
		194.1 (1)	10 and 11	198 (1)	27
		201.6 (2)		204 (2)	
		193.7		*198*	
$BeAl_2O_4$	C_i	186.2 (2)		194 (2)	
		189.2 (2)	10 and 11	197 (2)	
		191.7 (2)		200 (2)	
		189.0		*197*	

$10Dq$ values derived for the complex *in vacuo* and under the inclusion of $V_R(\mathbf{r})$ are both given. Figures for ruby and emerald coincide with those previously reported.[22] It should be noticed that under the suppression of $V_R(\mathbf{r})$ the calculated $10Dq$ values for the four centers look rather similar. For instance, the difference between calculated $10Dq$ values for the alexandrite (C_i center) and emerald is only about 700 cm^{-1}. This figure is, however, much smaller than the experimental figure equal to 4300 cm^{-1} as shown in Table III. Results gathered in Table III for complexes *in vacuo* underline that the small distortions of the CrO_6^{9-} octahedron in ruby, emerald, and the two Cr^{3+} centers in alexandrite have a small influence on the $10Dq$ value. Along this line, a calculation of a perfect CrO_6^{9-} octahedral complex *in vacuo* has also been carried out. For this octahedral complex with all Cr^{3+}-O^{2-} distances equal to 197 pm, it is found $10Dq = 16\,320$ cm^{-1}.

As a salient feature, results embodied in Table III stress that all differences in the experimental $10Dq$ values of the four Cr^{3+} centers can reasonably be understood once the effects of $V_R(\mathbf{r})$ upon the localized electrons in the CrO_6^{9-} unit are taken into account. In this sense the inclusion of $V_R(\mathbf{r})$ produces a supplementary increase of about 2000 cm^{-1} and 4000 cm^{-1} on the $10Dq$ values of C_s and C_i centers in alexandrite, respectively. In the case of ruby $V_R(\mathbf{r})$ leads to an increase of $10Dq$ similar to that for the C_s center in alexandrite. As regards emerald $10Dq$ undergoes however a small decrease when $V_R(\mathbf{r})$ is taken into account.

Some insight into these results can be obtained looking at the form of the $V_R(\mathbf{r})$ potential in the complex region. Results of $V_R(\mathbf{r})$ along the metal-ligand directions are portrayed in Figs. 1 and 2. Let us denote by x the distance of an electron to the impurity along one of such directions. It can firstly be noticed that in the case of emerald $V_R(x)$ is practically flat for $|x| < 1$ Å, thus explaining why the effects of

TABLE III. Calculated values of the ligand field parameter $10Dq$ for CrO_6^{9-} clusters *in vacuo* and considering the electrostatic potential from the rest of the lattice, V_R. Calculations have been performed to the experimental metal-ligand distance of each center. Experimental $10Dq$ values are given for comparison. All values are given in cm^{-1}.

System	Cluster *in vacuo*	Including V_R	Experimental	Refs.
Ruby	16043	18179	18070	1–3 and 6
Emerald	16188	15739	16130	1, 2, and 6
Alexandrite C_s	15682	17738	17700	3 and 7–9
Alexandrite C_i	16905	20864	20410	3 and 7–9

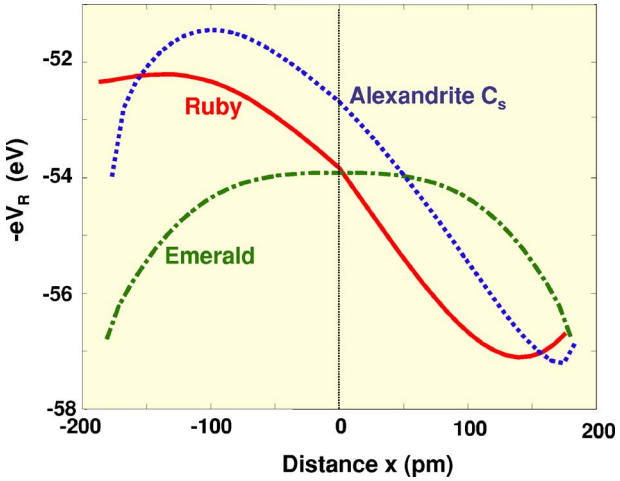

FIG. 1. (Color online) Electrostatic potential, $V_R(\mathbf{r})$, of the rest of lattice ions on CrO_6^{9-} along metal-ligand directions for ruby, emerald, and C_s center of alexandrite.

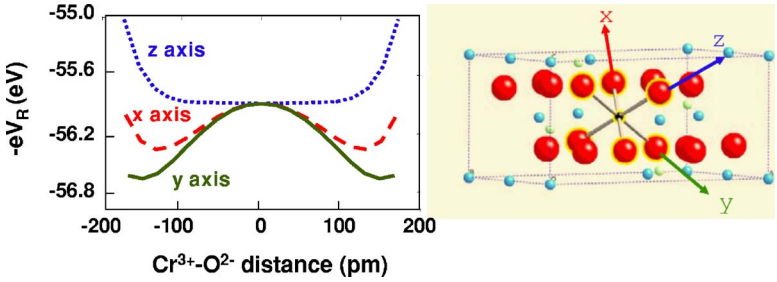

FIG. 2. (Color online) Left: Electrostatic potential, $V_R(\mathbf{r})$, of the rest of lattice ions on CrO_6^{9-} for the C_i center of alexandrite, depicted along the three metal-ligand directions shown at the picture on the right.

$V_R(\mathbf{r})$ upon $10Dq$ are found to be small in comparison with what is calculated for the other three centers in Table III. In these cases (Figs. 1 and 2) the plot of $V_R(x)$ exhibits a quite different behavior from that for $Be_3Si_6Al_2O_{18}$. It is worth noting that $V_R(x)$ for Al_2O_3 and the C_s center in $BeAl_2O_4$ look rather similar. This allows one to understand why the increase on $10Dq$ due to the influence of $V_R(\mathbf{r})$ in ruby and the C_s center in alexandrite are rather comparable. It has been pointed out that the electric field created around Cr^{3+} in these two centers polarizes the CrO_6^{9-} unit.[22] This implies an energy increase of the σ antibonding e_g level higher than that for the corresponding π antibonding t_{2g} level, leading to a supplementary increase of $10Dq$.

Huge differences are however found when comparing $V_R(\mathbf{r})$ for both the C_s center in alexandrite and ruby (Fig. 1) with that for the C_i center in alexandrite. In this case, although $V_R(x)=V_R(-x)$ for every metal-ligand direction (consistently with the existence of inversion symmetry), the form of $V_R(x)$ is quite sensitive to the considered direction. This special situation is not found in the other centers of Table I.

The non-flatness of $V_R(\mathbf{r})$ in the complex region induces different variations on the energy of antibonding e_g and t_{2g} orbitals. For this reason the influence of $V_R(\mathbf{r})$ on the optical spectrum is expected to appear mainly in transitions involving an excited state with a configuration *different* from t_{2g}^3 corresponding to the ground state. This happens for the $^4A_{2g}(t_{2g}^3) \rightarrow {}^4T_{2g}(t_{2g}^2 e_g)$ transition indeed but not in the case of $^2E_g \rightarrow {}^4A_{2g}(t_{2g}^3)$ transition responsible for the sharp emission line of Cr^{3+} in the four centers of Table I. In fact, the ^2E_g state is mainly built from the t_{2g}^3 configuration.[17] This simple argument thus explains why the emission energy E_{em} is found to be the same (within 2%) for ruby, emerald, and the two centers in alexandrite (Table I).

IV. FINAL REMARKS

It has been shown that the actual value of the $10Dq$ parameter for the two centers in alexandrite as well as for ruby and emerald can be well understood just considering the influence of the electrostatic potential, $V_R(\mathbf{r})$, from the rest of lattice ions upon the CrO_6^{9-} unit. It is worth noting that although $V_R(\mathbf{r})$ has not usually been taken into account in the traditional ligand field theory, the present results demonstrate that it plays a key role for explaining the *differences* displayed by the same complex but embedded in different host lattices.

A part of the contribution of $V_R(\mathbf{r})$ upon the final separation between e_g and t_{2g} orbitals can arise from the polarization of the CrO_6^{9-} complex due to internal electric fields. It should be remarked that this mechanism would also lead to changes on total charges and the covalency. First results indicate that for the two centers in alexandrite and ruby there is a slight increase in covalency when the effects of $V_R(\mathbf{r})$ are switched on. Further research along this line is now underway.

ACKNOWLEDGMENTS

Thanks are due to S. Watanabe and K. Ogasawara for their kind information on equilibrium distances in the C_s center of alexandrite. Partial support by the Spanish Ministerio de Ciencia y Tecnología under Projects No. MAT2005-00107 and No. FIS2006-02261 is acknowledged.

[1] K. Nassau, *The Physics and Chemistry of Colour* (John Wiley & Sons, New York, 1983).
[2] R. G. Burns, *Mineralogical Applications of Crystal Field Theory* (Cambridge University Press, Cambridge, 1993).
[3] R. C. Powell, *Physics of Solid-State Laser Materials* (Springer, New York, 1998).
[4] A. H. Jahren, M. B. Kruger, and R. J. Jeanloz, J. Appl. Phys. **71**, 1579 (1992).
[5] A. A. Payne, L. L. Chase, L. K. Smith, W. L. Kway, and H. W. Newkirk, J. Appl. Phys. **66**, 1051 (1989).
[6] E. Gaudry, Ph.D. thesis, Université Paris 6 (2004).
[7] K. L. Schepler, J. Appl. Phys. **56**, 1314 (1989).
[8] R. C. Powell, L. Xi, X. Gang, G. J. Quarles, and J. C. Walling, Phys. Rev. B **32**, 2788 (1985).
[9] A. Edgar, J. M. Spaeth, and G. J. Troup, Phys. Status Solidi A **88**, K175 (1985).
[10] A. P. Eliseev, A. M. Yurkin, and E. G. Samoilova, Phys. Status Solidi A **88**, K169 (1988).
[11] E. F. Farrel, J. H. Fang, and R. E. Newnham, Am. Mineral. **48**, 804 (1963).
[12] M. K. Rabadanov and P. Dudka, Crystallogr. Rep. **43**, 6 (1998).
[13] C. E. Forbes, J. Chem. Phys. **79**, 2590 (1983).
[14] T. H. Yeom and S. H. Choh, J. Appl. Phys. **90**, 5946 (2001).
[15] R. M. Fernandes Scalvi, M. Siu Li, and L. V. Scalvi, J. Phys.:

Condens. Matter **18**, R315 (2006).
[16] L. E. Orgel, Nature **179**, 1348 (1957).
[17] S. Sugano, Y. Tanabe, and H. Kamimura, *Multiplets of Transition-Metal Ions in Crystals* (Academic Press, New York, 1970).
[18] M. Moreno, M. T. Barriuso, J. A. Aramburu, J. M. García-Fernandez, and J. M. García-Lastra, J. Phys.: Condens. Matter **18**, R315 (2006).
[19] S. J. Duclos, Y. K. Vohra, and A. L. Ruoff, Phys. Rev. B **41**, 5372 (1990).
[20] E. Gaudry, A. Kiratisin, P. Sainctavit, C. Brouder, F. Mauri, A. Ramos, A. Rogalev, and J. Goulon, Phys. Rev. B **67**, 094108 (2003).
[21] E. Gaudry, P. Sainctavit, F. Juillot, F. Bondioli, Ph. Ohresser, and I. Letard, Phys. Chem. Miner. **32**, 710 (2006).
[22] J. M. García-Lastra, M. T. Barriuso, J. A. Aramburu, and M. Moreno, Phys. Rev. B **72**, 113104 (2005).
[23] K. Ogasawara, T. Ishii, I. Tanaka, and H. Adachi, Phys. Rev. B **61**, 143 (2000).
[24] G. te Velde, F. M. Bickelhaupt, E. J. Baerends, C. Fonseca Guerra, S. J. A. van Gisbergen, J. G. Snijders, and T. Ziegler, J. Comput. Chem. **22**, 931 (2001).
[25] J. P. Perdew, J. A. Chevary, S. H. Vosko, K. A. Jackson, M. R. Pederson, D. J. Singh, and C. Fiolhais, Phys. Rev. B **46**, 6671 (1992).
[26] J. A. Aramburu, J. M. García-Lastra, M. T. Barriuso, and M. Moreno, Int. J. Quantum Chem. **91**, 197 (2003).
[27] S. Watanabe and K. Ogasawara, private communication.
[28] J. A. Aramburu, M. Moreno, K. Doclo, C. Daul, and M. T. Barriuso, J. Chem. Phys. **110**, 1497 (1999).
[29] M. Atanasov, C. A. Daul, and C. Rauzy, Chem. Phys. Lett. **367**, 737 (2003).
[30] H. Adachi, S. Shiokawa, M. Tsukada, C. Satoko, and S. Sugano, J. Phys. Soc. Jpn. **47**, 1528 (1979).